AD-A127 813 POLY(VINYLIDENE FLUORIDE)(U) CASE WESTERN RESERVE UNIV 1/1
CLEVELAND OH DEPT OF MACROMOLECULAR SCIENCE
M H LITT ET AL. 1977 DAAR70-77-C-0055

UNCLASSIFIED F/G 11/9 NL

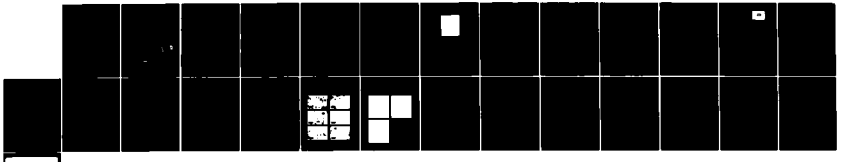

END
DATE FILMED
5 83
DTIC

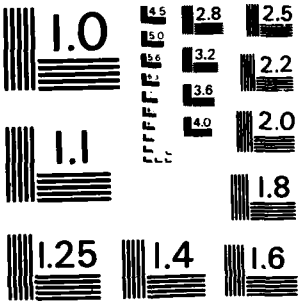

FINAL REPORT

DARPA Grant DAAK 70-77C-0055

POLY(VINYLIDENE FLUORIDE)

M. H. Litt and J. B. Lando

Department of Macromolecular Science
Case Western Reserve University
Cleveland, Ohio 44106

1977

83 05 02 103

POLY(VINYLIDENE FLUORIDE)

This project goal was to determine the maximum pyroelectric effect possible from poled poly(vinylidene fluoride) (PVF2). While much else was accomplished, which will be described below, we found no evidence that the pyrolectric coefficient of PVF2 could be made much higher than has already been achieved.

Achievements

The major achievements under this project were:

1. High molecular weight PVF2 and copolymers with vinyl fluoride VF were made. Control over molecular weight was established. H-H content was lower than in normal PVF2. This has been reported [M. H. Litt, S. Mitra and J. B. Lando, Macromolecules accepted].
2. The high molecular weight PVF2 was cast as a film, oriented at 180°C. and annealed at that temperature. Almost pure γ-PVF2 was obtained and its unit cell and crystal structure determined. This resulted in two papers [S. Weinhold, M. H. Litt and J. B. Lando, Polymer Letters 17, 585 (1979); S. Weinhold, M. H. Litt and J. B. Lando, Macromolecules 13, 1178 (1980)].
3. The nature of the surface for nucleation of PVF_2 in film form was studied. We had hoped to generate an oriented, non-centrosymmetric crystal form using epitaxial crystallization from the melt on metal (or metal oxide) surfaces. Under our crystallization conditions, the α-crystal form with the b axis perpendicular to the surface, [The

PVF_2 dipole is then parallel to the film surface) was generated, which is the non-polar form. [Copolymers which crystallize spontaneously in polar forms should have been studied too.] This resulted in a paper [S. Weinhold, M. H. Litt and J. B. Lando, J. Appl. Phys. 51, 5145 (1980)].

4. We have studied the pyroelectric properties of commercial, poled PVF2 as a function of annealing and cycling conditions. Poled Pennwalt film acts very differently from Kureha film. Both show crystallization of low melting PVF_2 on standing at room temperature which remelts at about 50-60°C during heating. A manuscript is in preparation [J. Bates, M. H. Litt, S. Weinhold and J. B. Lando - Anomalous Pyroelectric Response of Poled PVF2 as a Function of Aging.]

5. The melting and annealing behavior of our synthesized PVF_2 was compared to that of commercially produced materials, as our material had little H-H structure and no contaminating material. We found that our materials recrystallized faster than the commercial materials, but annealled Tm's were all close. We postulated that our materials had less branching which allowed them to reach higher Tm's and higher % crystallinity in a short time, compared to commercial materials. A paper has been written. [S. Weinhold, J. B. Lando and M. H. Litt - The Melting Behavior of Poly(vinylidene Fluoride].

6. It is well known that poling of α-form PVF2 can generate a δ, polar form. We have studied the poling of our directionally crystallized α-PVF_2, where the PVF_2 dipole is originally parallel to the surface. While this poles, it does so poorly with the possible formation of a poorly crystalline new phase in addition to the δ phase. This is being written up. [S. Weinhold, M. H. Litt and J. B. Lando - no title decided]

Personnel

The personnel on this project were mainly postdoctoral fellows. D. S. Mitra and Dr. J. Bates worked on this. The major graduate researcher was Steven Weinhold. As is obvious from the paper authors, he was the most productive member of the team. He received his M.S. degree in 1981 and will get his Ph.D. degree early in 1982. He was supported on the DARPA grant until it expired, and has continued the research since.

Papers

A copy of each of the published papers is appended.

ORIENTED PHASE III POLY(VINYLIDENE FLUORIDE)

Introduction

Three crystal forms of poly(vinylidene fluoride) (PVF_2) are known. Phase I, or the β phase, has been shown to consist of planar (or nearly planar) zig-zag chains packed into an orthorhombic unit cell (1,2) with dimensions a = 0.858 nm, b = 0.491 nm, and c (chain direction) = 0.256 nm. Phase II, or the α phase, is composed of chains with an approximate trans-gauche-trans-gauche' backbone rotation sequence (2,3). The unit cell is probably monoclinic (2,3) [but perhaps triclinic (3)] with all unit-cell angles equal to 90° within experimental error, and with cell dimensions a = 0.496 nm, b = 0.964 nm, and c (fiber axis) = 0.462 nm.

Phase III, or the γ phase, very readily undergoes a crystal-crystal phase transition to phase I when mechanically deformed (4-6). Thus, Hasegawa et al. (2) used unoriented samples to determine their proposed structure for phase III. According to Hasegawa et al. (2) the phase III chain conformation is identical to that in phase I; that is, an essentially all-trans backbone. However, the interchain packing is slightly different in the two crystal phases, resulting in a monoclinic unit cell for phase III with dimensions a = 0.866 nm, b = 0.493 nm, and c (chain direction) = 0.258 nm with the monoclinic angle $\beta = 97°$.

We have recently succeeded in preparing well-oriented phase-III PVF_2. This communication presents our interpretation of data obtained from oriented films, which differs from that of Hasegawa et al.

Results and Discussion

To synthesize the PVF_2, vinylidene fluoride gas was double-distilled under vacuum into a Paar stainless-steel vacuum and pressure-tight bomb, where it was frozen and degassed several times. The bomb was then placed into an ice bath at 0°C and irradiated with ^{60}Co γ radiation. The viscosity of the resulting polymer was measured in N,N-dimethylacetamide (DMA) at 30.0°C using an Ubbelohde dilution viscometer. The intrinsic viscosity ranged from 5 to 8 dl/g, showing that the polymer has an extremely high molecular weight.

Films of this PVF_2, approximately 20-25 μm thick, were produced by casting a DMA solution onto glass plates and evaporating the solvent at 90-110°C. The films were then stripped from the glass, soaked in acetone to extract any remaining DMA, and then heated to 90-110°C under vacuum. Infrared spectra of the resulting films showed the complete absence of characteristic phase I and phase II absorption bands (4,5). Prest and Luca (5) reported that weak bands at 430, 776, and 810 cm^{-1} are characteristic of phase III, while Kobayashi et al. (4) observed that a strong band at 1230 cm^{-1}, accompanied by a weak band at 1273 cm^{-1} is distinctive of phase III. These bands were present

Journal of Polymer Science: Polymer Letters Edition, Vol. 17, 585-589 (1979)
 0360-6384/79/0017-0585$01.00

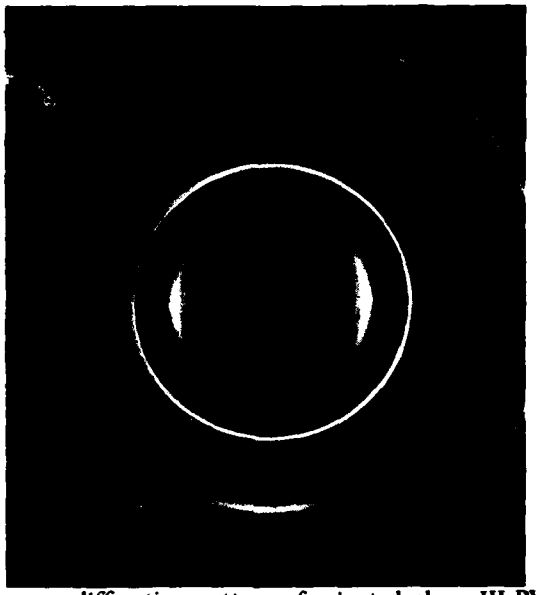

Fig. 1. The x-ray diffraction pattern of oriented phase III PVF_2. The rings are caused by CaF_2 on the sample.

in the infrared spectra of the films cast from DMA, making it apparent that only phase III was present. This was the expected result, as it has been previously reported that PVF_2 crystallizes into phase III out of DMA solution (4). Also, no trace of solvent could be seen in the films. X-ray diffraction patterns showed the complete absence of phases I and II. The peak of the DSC melting endotherm occurred at 178°C for these films.

X-ray diffraction patterns were obtained using CuKα radiation with a flat plate Statton camera purged with helium. Sample-to-film distances were determined by dusting the sample with CaF_2. IR spectra were taken with a Digilab FTS-14 Fourier transform infrared spectrometer. DSC data were obtained using a Perkin-Elmer DSC-2 apparatus. Samples were drawn with an Instron tensile tester.

Oriented samples were prepared by drawing a dogbone-shaped piece of film at approximately 178°C at a draw rate of 10%/min to a draw ratio of about 5 and then cooling it slowly under tension. The infrared spectrum of the drawn samples showed the predominant presence of phase III (4,5). This was concluded from the strength of the characteristic phase III bands discussed above. A small amount of phase I was also detected (4,5). No absorption bands characteristic of phase II (4,5) were seen.

Figure 1 shows the x-ray diffraction pattern of such a drawn PVF_2 cast film. Figure 2 shows a sketch of the diffraction pattern with the indexing of the reflections indicated. All reflections other than the phase I reflections could be indexed assuming an orthorhombic unit cell with dimensions a =

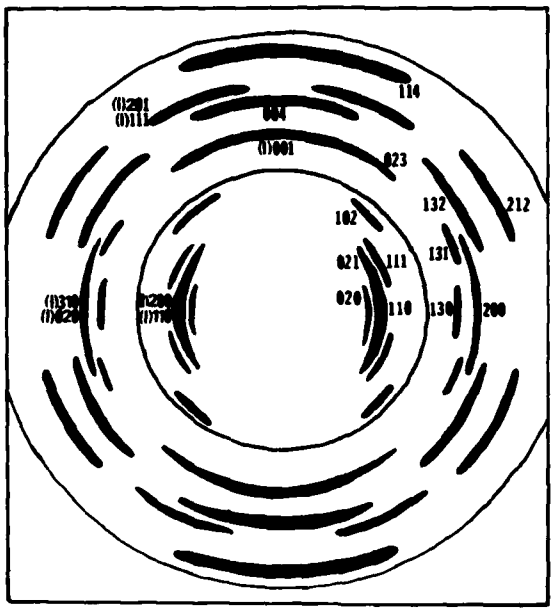

Fig. 2. A sketch of the x-ray diffraction pattern of oriented phase III PVF_2. Indices of the reflections are shown. Indices preceded by (1) indicate phase I reflections.

0.497 nm, b = 0.966 nm, and c (chain direction) = 0.918 nm. Table I lists the observed and calculated d spacings and their indexing. Several equatorial reflections have d spacings corresponding to phase I equatorial reflections. Reflections with these spacings are also observed on the diffraction pattern of unoriented cast film, which contains no phase I. Hence, these reflections are unambiguously present in the phase III diffraction pattern. We note that the a and b dimensions of the phase III unit cell are almost exactly equal to the corresponding phase II unit-cell dimensions, while the c repeat distance is essentially double that of the phase II c repeat.

At the present time, we have x-ray diffraction data extending out to a d spacing of about 0.16 nm. Hasegawa et al. (2) observed reflections at seven d spacings in this interval for unoriented phase III films cast from dimethylsulfoxide solution. We also observe reflections at these seven d spacings (within experimental error) as well as reflections at several other spacings. Furthermore, the data of Hasegawa et al. at spacings less than 0.16 nm can also be indexed using the unit cell proposed here. Thus, all the data of Hasegawa et al. are consistent with this unit cell.

A number of chain conformations can be postulated which have a 0.918-nm repeat distance. However, an essentially all-trans backbone as proposed by Hasegawa et al. for phase III does not have this repeat. That the phase III structure should be related more to phase II than to phase I is not unreason-

TABLE I

Observed and Calculated d Spacings and Indexing of the X-Ray Diffraction Pattern of Oriented Phase III PVF_2

Obs., nm	Calc.[a], nm	h k ℓ
0.480	0.483	020
0.442	0.442	110
0.271	0.270	130
0.248	0.249	200
0.176	0.173	240
0.162	0.163	310
	0.161	060
0.431	0.427	021
0.395	0.398	111
0.258	0.259	131
0.336	0.337	102
	0.333	022
0.237	0.233	132
0.214	0.214	042
	0.213	212
0.168	0.168	152
0.260	0.259	023
0.230	0.230	004
0.201	0.204	114

[a]Spacings calculated from the unit cell of phase III (a = 0.497 nm, b = 0.966 nm, c = 0.918 nm).

able considering the fact that high-temperature annealing induces a transition of phase II to phase III, but not a transition of phase I to phase III (5).

Most of the possible phase III chain conformations exhibit a net dipole moment. Also, systematic absences in the observed reflections show conclusively that an n-glide perpendicular to the c axis of the unit cell is present. (For hk0 reflections, h + k = odd are absent.) If the phase III chain does, in fact, possess a net dipole, the presence of this glide plane dictates that the two chains in the unit cell be oriented so that their dipole moments are parallel. These considerations strongly suggest that the phase III unit cell could possess a net dipole moment.

We are currently determining the detailed crystal structure of phase III PVF_2. Our results will be published in the near future.

This research was partially supported by the Defense Advanced Research Projects Agency and monitored by the Army Night Vision Laboratory under Contract No. DAAK 70-77-C-0055.

References

(1) J. B. Lando, H. G. Olf, and A. Peterlin, J. Polym. Sci. A-1, 4, 941 (1966).

(2) R. Hasegawa, Y. Takahashi, Y. Chatani, and H. Tadokoro, Polym. J., 3(5), 600 (1972).

(3) W. W. Doll and J. B. Lando, J. Macromol. Sci. Phys., 4(2), 309 (1970).

(4) M. Kobayashi, K. Tashiro, and H. Tadokoro, Macromolecules, 8, 158 (1975).

(5) W. M. Prest, Jr. and D. J. Luca, J. Appl. Phys., 46(10), 4136 (1975).

(6) R. Hasegawa, M. Kobayashi, and H. Tadokoro, Polym. J., 3(5), 591 (1972).

S. Weinhold
M. H. Litt
J. B. Lando

Department of Macromolecular Science
Case Western Reserve University
Cleveland, Ohio 44106

Received November 8, 1978
Revised February 9, 1979

Macromolecules **1980**, *13*, 1178–1183

The Crystal Structure of the γ Phase of Poly(vinylidene fluoride)

S. Weinhold, M. H. Litt, and J. B. Lando*

Department of Macromolecular Science, Case Institute of Technology, Case Western Reserve University, Cleveland, Ohio 44106. *Received January 18, 1980*

ABSTRACT: The crystal structure of the γ phase of poly(vinylidene fluoride) (PVF_2) was determined by X-ray diffraction techniques. Oriented specimens of the γ phase were obtained by high-temperature drawing of films of ultrahigh molecular weight PVF_2 cast from dimethylacetamide solution. The unit cell of the γ phase was found to be orthorhombic with dimensions $a = 0.497$, $b = 0.966$, and $c = 0.918$ nm. The chain conformation is approximately TTTGTTTG′. Individual chains with this conformation possess a net electrical dipole and pack such that the unit cell is polar. The chains pack in a statistical parallel–antiparallel manner, which can be modeled by a hypothetical four-chain unit cell belonging to space group *C2cm*.

Four crystal forms of poly(vinylidene fluoride) are known. The α phase, or phase II, is the form produced by crystallization from the melt at atmospheric pressure[1] at normal degrees of supercooling.[2] The chain conformation of the α phase has been shown[3,4] to be approximately trans–gauche–trans–gauche′. The unit cell has been reported as being monoclinic[3,4] (or triclinic[4]) with all unit cell angles equal to 90°, within experimental error, and with cell dimensions of $a = 0.496$, $b = 0.964$, and $c = 0.462$ nm. While individual chains of the α phase possess a net electrical dipole, the two chains in the unit cell pack such that their dipoles exactly cancel, resulting in a nonpolar unit cell.

Several authors[5-7] have recently reported evidence suggesting the existence of a polar version of the α phase, which is produced by subjecting a film of α-PVF_2 to a moderately strong poling field. While no detailed structure analysis of this form has been published, it is generally believed that the chain conformation and the unit cell dimensions are similar to that of the α phase and that the two chains in the cell pack such that their dipoles reinforce rather than cancel one another.

The third known polymorph of PVF_2 is known as the β phase, or phase I. It is most commonly prepared by relatively low temperature mechanical deformation of the α phase.[1,8] The β phase has been shown[1,3] to consist of planar (or nearly planar) zigzag chains packed into an orthorhombic unit cell with dimensions $a = 0.858$, $b = 0.491$, and $c = 0.256$ nm.

The last known polymorph of PVF_2 is known as the γ phase, or phase III. The techniques which have been reported to yield this crystal phase include the following: crystallization from the melt at high temperatures and pressures;[8,9] annealing the α phase at high temperatures and pressures;[8] various atmospheric-pressure thermal treatments of both the α[2,10,11] and β[10] phases; high-temperature crystallization from the melt at atmospheric pressure;[12] and crystallization from dimethyl sulfoxide, dimethylacetamide (DMA), and dimethylformamide solutions.[13-15]

The γ phase very readily undergoes a crystal–crystal phase transition to the β phase when mechanically deformed.[2,8,9] Thus, Hasegawa et al.[3] used unoriented samples to determine their proposed structure for the γ phase. According to Hasegawa et al.,[3] the γ-phase chain conformation is identical with that in the β phase, that is, a nearly all-trans backbone. However, it was proposed that the interchain packing is slightly different in the two crystal phases, resulting in a monoclinic unit cell for the γ phase with dimensions $a = 0.866$, $b = 0.493$, and $c = 0.258$ nm with the monoclinic angle $\beta = 97°$.

In a previous publication[16] we reported a different unit cell for the γ phase of PVF_2. On the basis of X-ray fiber diffraction patterns, we determined that the unit cell of γ-PVF_2 was orthorhombic with dimensions $a = 0.497$, $b = 0.966$, and c (chain direction) = 0.918 nm. We noted that the c-axis repeat distance was incompatible with the essentially all-trans chain conformation proposed by Hasegawa et al.[3] This unit cell has since been confirmed by electron diffraction experiments performed with high-temperature melt-crystallized γ-PVF_2.[12] Also, a detailed infrared study[17] has shown that the crystalline IR spectrum of γ-PVF_2 is much more complicated than was previously believed and has thus demonstrated that the chain conformation cannot be essentially all trans. In addition, a conformational energy analysis has been performed[18,19] with the goal of predicting the major features of the chain conformation of the γ phase.

In this paper we discuss the crystal structure of the γ phase of PVF_2 as determined by X-ray diffraction techniques.

Experimental Section

Specimen Preparation. The preparation of uniaxially oriented films of γ-PVF_2 has been discussed in a previous paper.[16] However, a brief review is in order here. The PVF_2 used for this work was synthesized in our laboratory by a bulk polymerization at 0 °C initiated by ^{60}Co γ radiation. A detailed discussion of this synthesis technique is to be published.[20] The viscosity of this polymer was measured in DMA at 25 °C with an Ubbelohde dilution viscometer. The intrinsic viscosity [η] was determined to be 8.3 dL/g. The equation[21] $[\eta] = 1.93 \times 10^{-4} M^{0.677}$ was used in calculating the viscosity-average molecular weight as about 7×10^5. This value for the molecular weight must be considered as only a rough estimate, as [η] is outside the range for which the molecular weight–viscosity relationship was determined. Thin films of γ-PVF_2 were made by casting a DMA solution of this material onto glass plates. Oriented specimens were prepared by drawing these solution-crystallized films at 178 °C. Infrared spectra of the drawn films showed that they consisted predominantly of the γ-phase, but with a significant quantity of the β-phase also present.

X-ray Techniques. X-ray fiber diffraction photographs were taken with nickel-filtered Cu Kα radiation. A flat-plate camera was used to record the relatively low angle portion of the diffraction pattern, while a cylindrical camera with a diameter of 5[illegible]cm was used to record diffraction data occurring at larger angles. The cameras were purged with helium to minimize air scattering. The *d* spacings were calibrated by dusting the sample with CaF_2. Multiple film techniques were used for intensity measurements. The relative intensities of the diffraction maxima were measured by scanning the diffraction photographs with a Photometrics microdensitometer and storing the optical density

data on magnetic tape. These data were then computer processed to yield a large two-dimensional optical density matrix from which values for integrated spot intensity and background intensity could be determined. Also, a small amount of data was collected by taking radial densitometer scans of powder diffraction photographs. In addition the intensities of a number of spots, for the most part occurring at large diffraction angles, were determined visually. Corrections for Lorentz and polarization effects were applied. Absorption effects were calculated to be insignificant with respect to the probable error associated with the intensity data; therefore absorption corrections were not applied.

Finally, the effects of the significant quantity of the β phase present in all of the oriented specimens was taken into account. This was necessary because a number of γ-phase and β-phase *hk*0 reflections overlap. Assuming that the two crystal phases exist in crystallographically separate domains, the relative quantity of the β phase was determined from the intensity of the β-phase 201, 111 and 330, 600 spots. These two spots were chosen because overlap with a γ-phase spot is not possible. The β-phase contribution was then subtracted from the total intensity of overlapping spots, using the observed relative intensities for the β phase reported by Hasegawa et al.[3]

Refinement Methods

This structure was refined by using the LALS (linked-atom least-squares) mark 6 computer refinement program, which has been developed and described by Smith and Arnott.[22] The use of LALS makes possible the refinement of bond angles, internal rotation angles, intermolecular packing parameters, and scale and isotropic temperature factors. As in any structure refinement routine, LALS bases the structure refinement on observed structure factor amplitudes; however, undesirably short nonbonded interatomic contacts are also considered in the refinement. In addition, bond angles and internal rotation angles can be refined against the restraint that they be stereochemically reasonable.

The structure under discussion was determined in the following general manner. Because the fiber repeat distance is relatively large, a number of stereochemically reasonable chain conformations were possible. To determine which conformation was the correct one, a trial model for each conformation was treated as a rigid body and the interchain packing was refined within the constraints ir ed by the known symmetry. This was followed by a limited refinement of bond and internal rotation angles. A full refinement of the most promising conformation was then carried out.

The structure refinement is discussed in terms of the residuals

$$R' = \frac{\sum_{m=1}^{M} w_m^{1/2} ||F_m(\text{obsd})| - |F_m(\text{calcd})||}{\sum_{m=1}^{M} w_m^{1/2} |F_m(\text{obsd})|}$$

$$R'' = \left[\frac{\sum_{m=1}^{M} w_m ||F_m(\text{obsd})| - |F_m(\text{calcd})||^2}{\sum_{m=1}^{M} w_m |F_m^2(\text{obsd})|} \right]^{1/2}$$

where F_m(obsd) and F_m(calcd) are, respectively, the observed and calculated structure factor amplitudes for the *m*th of *M* reflections and w_m is a weighting factor. R'' is the more statistically meaningful of the two residuals and the bulk of the refinement was based upon this quantity. However, most of the residuals reported in the literature are R', so this quantity is reported here as well.

For this work the residuals are reported with $w = 1$ for all reflections; however, it was found that assigning a greater weight to those reflections for which $\Delta F/F$(obsd) was large often accelerated the refinement, so this was sometimes done.

Unobserved reflections, also known as less-thans, are those reflections which are not systematically absent because of the symmetry of the structure but are too weak with respect to the background intensity to be observed on the X-ray photograph. The unobserved data were, for the most part, not used in the actual refinement of this structure because of the extreme difficulty in determining an accurate threshold intensity, which varies from place to place on the diffraction photograph. The only circumstance in which an unobserved reflection was used in the refinement was when the calculated intensity of that reflection was great enough to leave little doubt that if that reflection were indeed the intense, it would be observable. In such a case the unobserved reflection was treated precisely the same as an observed reflection with an observed intensity equal to the threshold value. The unobserved data were, however, of very great importance in choosing between different models for the structure.

LALS is capable of calculating structure factors only for reflections with $d \geq 0.125$ nm. Hence, several observed reflections with spacing less than this limit were not used in refining the structure. The structure factors for these reflections, as well as those of unobserved reflections with spacings between 0.125 and 0.100 nm, were calculated with a different computer program, using the refined atomic coordinates supplied by LALS.

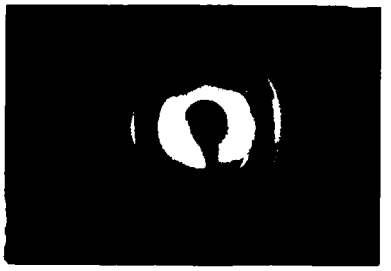

Figure 1. X-ray diffraction pattern of oriented γ-phase PVF_2.

Table I
Comparison between Observed and Calculated *d* Spacings of the γ Phase of PVF_2

d_{obsd}, nm	d_{calcd},[a] nm	*hkl*	d_{obsd}, nm	d_{calcd},[a] nm	*hkl*
0.480	0.483	020		0.106	370
0.442	0.442	110	0.106	0.105	190
0.271	0.270	130		0.105	371
0.248	0.248$_5$	200	0.431	0.427	021
	0.180	150	0.395	0.398	111
0.176	0.177	151	0.258	0.259	131
	0.173	240	0.336	0.333	022
	0.163	310		0.233	132
0.162	0.161	060	0.237	0.240	201
	0.161	311		0.234	041
	0.159	061	0.214	0.214	042
	0.135	260		0.215	221
0.132	0.134	261	0.168	0.168	152
	0.133	170		0.170	241
	0.132	171	0.160	0.162	242
	0.121	080	0.260	0.259	023
0.120	0.120	420	0.230	0.229$_5$	004
	0.120	081	*0.201*	*0.204*	114
	0.119	421			
	0.110$_5$	440			
0.109	0.110	441			
	0.109	280			
	0.108	281			
	0.107$_4$	442			

[a] Spacings calculated from the unit cell of the γ phase of PVF_2 (a = 0.497, b = 0.966, and c = 0.918 nm).

Structure Analysis and Results

A fiber diffraction photograph of the γ phase of PVF_2 is shown in Figure 1. Reflections due to the significant amount of β phase in the specimen are also present. In addition, several reflections due to CaF_2 are visible. The *d* spacings of the reflections attributed to the γ phase are shown in Table I and are indexed using an orthorhombic unit cell with dimensions a = 0.497, b = 0.966, and c (chain direction) = 0.918 nm. Due to the rather large c repeat distance and the imperfect orientation, it is impossible in several cases to resolve reflections on adjacent layer lines with very similar *d* spacings. These sets of reflections were

treated as overlapping reflections throughout the refinement.

The dimensions of the a and b axes, which are virtually identical with those of the α phase, indicate that a unit cell contains two chains. The length of the c axis, which is just slightly less than twice the length of the α-phase c axis, and the presence of a strong 004 reflection on the diffraction photograph show that the unit cell contains eight monomer units in the two chains. The calculated crystalline density is 1.92_8 g/cm^3, which is essentially identical with the calculated density of the α phase.

All of the observed reflections can be indexed such that the sum of the h and k indices is evenly divisible by 2; this is the condition for a C-centered unit cell. However, many of the upper layer reflections could also be indexed such that the above condition was not true, while almost none of the $hk0$ reflections could be indexed such that $h + k$ = odd. Thus, there was a possibility that the operative symmetry operation was an n glide normal to the c axis rather than C centering.

Either of these symmetry operations require that, if an atom on one chain exists at a position x, y in the unit cell, an identical atom on the other chain must exist at position $x + {}^1/_2, y + {}^1/_2$. Also, in physical terms a C-centered structure would mean that the two chains in the unit cell were of the same sence, that is, parallel. On the other hand, an n glide normal to c would require the two chains to be antiparallel.

The presence of either of these symmetry elements makes it highly probable, but not absolutely necessary, that a c glide normal to the b axis is also present. Only two chain conformations exist which are consistent with a c glide normal to b and which can be made to have the proper repeat distance. These conformations are those which have backbone internal rotation angle sequences of TTTGTTTG′ or TGTGTG′TG′. The fact that the a and b dimensions of the γ-phase unit cell are essentially identical with those of the α phase indicates that the chain conformation of the γ phase must be such that the interchain packing is very similar to that in the α phase. This consideration favors the TTTGTTTG′ conformation. Also, an infrared study of the γ phase performed by Bachmann et al.[17] favors this conformation as well. Finally, conformational energy calculations[18,19] also point to this conformation.

The conformations investigated in this work included the two mentioned above, TTTGTTTG′ and TGTGTG′TG′, as well as a third conformation with internal rotation angles of TTTTTGTG′. Other possible conformations were not considered here because the conformational energy calculations[18,19] showed them to be quite unfavorable.

In the course of the structure determination, it was found that neither the TGTGTG′TG′ conformation nor the TTTTTGTG′ conformation could be refined to give an acceptably low residual. They were therefore discarded as possibilities. The same was true of two parallel chains with a TTTGTTTG′ conformation. A structure consisting of antiparallel chains with such a conformation could be refined to give an acceptably low residual R' of about 0.18, calculated using only the observed reflections. However, for this model the intensities of a large number of experimentally unobserved reflections were calculated to be quite large. For example, the intensities of several unobserved reflections were calculated to be about 40 times that of the estimated threshold intensity. This drastic disagreement required that the model be discarded as a possibility.

Table II
Atomic Coordinates of the γ Phase of PVF_2

atom[a]	x/a	y/b	z/c
C_2	0.493	0.505	0.862
C_3	0.549	0.371	0.777
C_4	0.451	0.372	0.618
C_5	0.544	0.498	0.528
F_3	0.442	0.254	0.830
F_4	0.811	0.339	0.770
F_5	0.431	0.618	0.569
F_6	0.809	0.521	0.538
H_1	0.617	0.584	0.810
H_2	0.286	0.530	0.833
H_3	0.515	0.282	0.555
H_4	0.233	0.371	0.606

[a] Numbering of atoms is shown in Figure 2.

Table III
Molecular Dimensions of the γ Phase of PVF_2

Bond Lengths (nm)			
all C-C	0.154	all C-H	0.109
all C-F	0.134		
Bond Angles (Deg)			
C_1-C_2-C_3[a]	117.3	C_1-C_2-H_1	110.6
C_2-C_3-C_4	114.7	C_1-C_2-H_2	113.5
C_3-C_4-C_5	115.0	C_3-C_4-H_3	114.0
C_4-C_5-C_6	118.0	C_3-C_4-H_4	114.0
C_2-C_3-F_3	117.1	F_3-C_3-F_4	102.2
C_2-C_3-F_4	113.3	F_5-C_5-F_6	104.1
C_4-C_5-F_5	114.1	H_1-C_2-H_2	105.7
C_4-C_5-F_6	112.9	H_3-C_4-H_4	103.5
Internal Rotation Angles (Deg)			
C_1-C_2-C_3-C_4	170.4	C_3-C_4-C_5-F_5	−68.9
C_2-C_3-C_4-C_5	51.5	C_3-C_4-C_5-F_6	49.7
C_3-C_4-C_5-C_6	170.4	C_2-C_3-C_4-H_3	172.2
C_4-C_5-C_6-C_7	171.5	C_2-C_3-C_4-H_4	−69.3
C_1-C_2-C_3-F_3	49.7	C_4-C_5-C_6-H_5	−67.8
C_1-C_2-C_3-F_4	−68.9	C_4-C_5-C_6-H_6	50.8

[a] Numbering of atoms is shown in Figure 2.

On the basis of this knowledge, the structure of the γ phase was ultimately determined to consist of chains with a TTTGTTTG′ conformation packed in a statistical parallel–antiparallel manner. The occurrence of statistical packing in semicrystalline polymers is well established. In statistical parallel–antiparallel packing, the two chains in any given unit cell are either parallel or antiparallel, but different unit cells within the same crystallite may have either type of packing. For computational purposes this may be modeled by assuming a hypothetical unit cell in which two fractionally weighted chains, one of each sense, are placed at each chain position in the unit cell. For this work it was assumed that parallel packing and antiparallel packing occur with equal probability. Hence, this structure is modeled as a unit cell containing two up chains and two down chains, with the scattering factor for each atom divided by a factor of 2.

On the basis of zero-layer X-ray data, which are not dependent on the sense of the chains, it was determined that the TTTGTTTG′ conformation was the only possibility. A refinement of the chain conformation and the interchain packing was performed.

The atomic coordinates of an asymmetric unit, which consists of two monomer units, are given in Table II. Details of an individual chain with the numbering of the atoms indicated is shown in Figure 2. All intrachain, nonbonded atomic distances less than the sum of the van der Waals radii of the two atoms are also shown in Figure 2a. The van der Waals radius of a fluorine atom is taken to be 0.135 nm, while that of a hydrogen atom is taken as

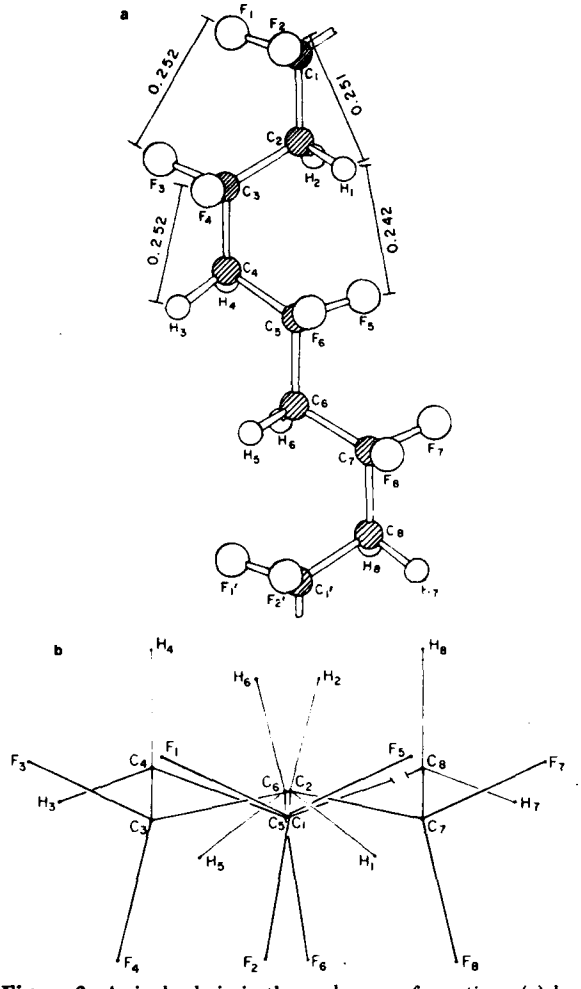

Figure 2. A single chain in the γ-phase conformation: (a) *bc* projection; (b) *ab* projection. Distances shown are in nm.

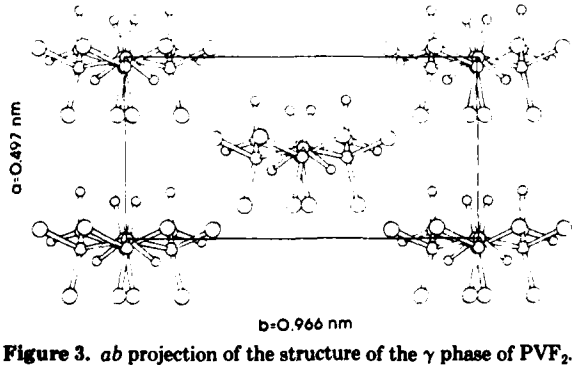

Figure 3. *ab* projection of the structure of the γ phase of PVF_2.

0.120 nm. The worst contact is between two fluorine atoms in the trans segment of the chain. The distance of 0.252 nm is quite close, but not bad enough to dismiss the possibility of its occurring. The molecular dimensions of this chain are given in Table III. Backbone bond angles range from about 115 to 118°, while trans backbone internal rotation angles are about 170° and the gauche angle is about 52°. An estimate of the degree of uncertainty associated with these parameters is ±1° for the bond angles and probably somewhat more than this for the rotation angles. Uncertainty estimates given for this work are in

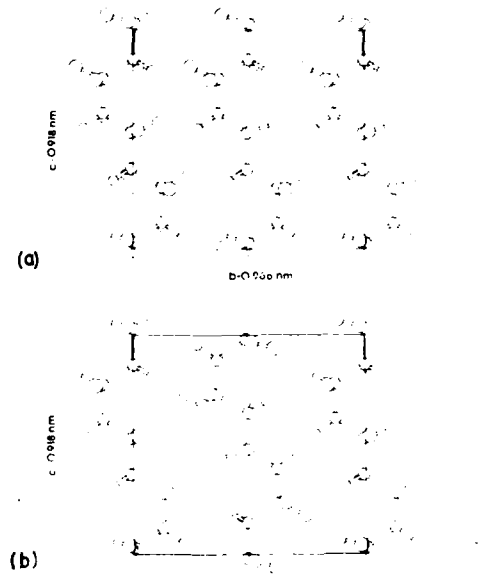

Figure 4. *bc* projections of the structure of the γ phase of PVF_2 demonstrating the packing of (a) parallel chains and (b) antiparallel chains.

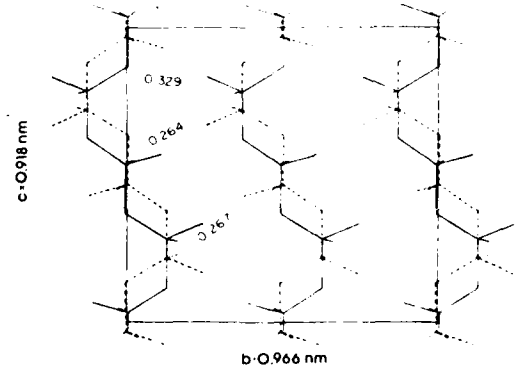

Figure 5. Sketch of the *bc* projection of the hypothetical four-chain unit cell used to model the structure of the γ phase of PVF_2. Solid lines illustrate chains with one sense and dashed lines illustrate chains with the opposite sense. Distances shown are in nm.

no way well-defined mathematical quantities. They are included to give some indication of the range in value which a parameter may adopt without serious detriment to the X-ray residuals and/or nonbonded interatomic contacts.

An *ab* projection of the structure is shown in Figure 3. Because the atoms of the two chains of opposite sense at the same position in the unit cell exactly overlap in this projection, only two chains are evident. Figure 4 shows the *bc* projections of parallel and antiparallel chains. Figure 5 shows a sketch of the *bc* projection of the cell with up and down chains at each position. Hydrogen atoms have been omitted for clarity. The dotted lines point out the three close interchain contacts. Taking the van der Waals radius of a fluorine atom to be 0.135 nm and that of a methylene group to be 0.200 nm, the closest contact is 0.006 nm short of the sum of the van der Waals radii, a relatively insignificant amount.

We have chosen to define the interchain packing as we have because of the very high symmetry of the resulting structure. The space group for this hypothetical four-chain unit cell structure is $C2cm$ (No. 40[23]). All four chains are

Table IV
Comparison between Observed and Calculated Structure Factor Amplitudes of the γ Phase of PVF_2

hkl[a]	$\|F_o\|$[b]	$\|F_c\|$[c]	hkl	$\|F_o\|$	$\|F_c\|$
020	38.1	36.9	442		
110	very strong[d]	175.0	280	74.8	70.9
021			441		
130	19.6	22.3	440		
200	108.3	97.9	281		
151			190		
150	74.9	85.3	370	52.6	43.7
240			371		
310			111	81.3	89.6
311	114.1	108.9	131	55.4	55.7
060			022	122.2	122.4
061			132		
171			041	183.8	143.2
170			201		
260	63.7	56.8	042	102.8	44.4
261			221		
080			152	42.3	50.0
421			241		
420	70.0	62.6	242	43.5	46.2
081			023	78.6	89.0
			114	32.5	83.4

[a] In the case of overlapping reflections, the planes contributing to that spot are listed such that the plane with the greatest calculated contribution to the intensity of the spot is listed first, the plane with the second greatest calculated contribution is listed second, etc. [b] The observed structure factor amplitude is $k(I_{obsd})^{1/2}$, where I_{obsd} is the observed relative intensity and k is the scale factor. The calculated structure factor amplitude is $(mF_c^2)^{1/2}$, where m is the multiplicity and F_c is the calculated structure factor. For overlapping reflections this value is $(\Sigma mF_c^2)^{1/2}$. [d] This spot was not considered in the structure refinement; see text.

generated by symmetry from the asymmetric unit consisting of two monomer units. The residual can be slightly decreased by changing the relative shift of the two parallel chains along the c axis or by slightly rotating the chains about their axes. However, these changes would drastically reduce the symmetry of the structure. The slight decrease in the residual produced by these changes is not statistically significant, considering the additional degrees of freedom made available by reducing the symmetry. Estimates for the uncertainty associated with the packing parameters are as follows: ±0.005c for the relative shift along c between antiparallel chains, ±0.03c for the shift between parallel chains, and ±2° for the rotation of the chains about a line parallel to the c axis that might be considered to be the chain axis. As the chains are not helical, they do not posses a precisely defined chain axis.

Table IV lists calculated vs. observed structure factor amplitudes for all of the observed reflections. The calculated values were computed with the overall isotropic temperature factor B = 3.75 Å^2. The temperature and scale factors were refined parameters and have an estimated uncertainty of ±0.25 Å^2 for B and ±3% for the scale factor. The 110,021 spot was not considered in the refinement because an accurate determination of its intensity was impossible for two reasons. First, it is the strongest reflection on the diffraction pattern and thus is difficult to scale to weaker spots. The greatest cause of uncertainty, however, was overlap with the very intense β-phase 110,200 spot. Nonetheless, the γ-phase 110,021 reflection has a greater calculated intensity than any other reflection, in agreement with experiment.

For this work, the observed intensity was defined to be the sum of the intensities of all of the spots on the diffraction pattern with the same *hkl*. This is contrary to the conventional definition, where the observed intensity is taken to be the average intensity of one of these spots. It was necessary to define observed intensity in this manner because of the overlap between zero-layer reflections, for which there are two equivalent spots, and first-layer reflections, for which there are four equivalent spots.

The residuals for this structure, based on all the observed data except the 110,021 reflection, are R' = 0.174 and R'' = 0.253. The agreement for unobserved reflections is also quite good, with only a few unobserved reflections having a calculated intensity greater than the estimated threshold intensity. A residual incorporating unobserved reflections can be calculated by ignoring those reflections with a calculated intensity less than the threshold and treating those reflections with a calculated intensity greater than the threshold as observed reflections with an observed intensity equal to the threshold.

The residual calculated from both the unobserved reflections and the observed reflections (except the 110,021), with unity weight assigned to each reflection, was R' = 0.218. For comparison, this residual for the nonstatistical, antiparallel-chain model mentioned previously was 0.50.

Discussion

There exists a considerable body of literature concerned with the high-pressure crystallization of poly(vinylidene fluoride).[8,9,24-27] However, the results of these experiments are confused, with some authors[8,9] reporting the formation of the γ phase and other investigators[24,25] reporting the formation of the α and/or β phase under similar conditions. As X-ray diffraction was the predominant technique used to identify the crystal phases present in these samples, some of this confusion may be due to the incorrect γ-phase unit cell proposed by Hasegawa et al.[3]

The crystal structure of the γ phase presented here also sheds light on the thermally induced α-phase to γ-phase transition. It has been shown[2,10,11] that annealing melt-crystallized α-phase spherulites close to their melting temperature results in a solid-state transition from the α phase to the γ phase. However, a solid-state transition from the β phase to the γ phase does not occur.[10] This behavior is somewhat difficult to explain if the γ phase is considered to be a minor modification of the β phase, as proposed by Hasegawa et al.[3] On the other hand, this behavior seems quite reasonable in light of the great similarity in the chain packing of the α phase and the γ phase described in this report.

Similarly, the γ-phase to β-phase solid-state transition, which occurs very readily upon mechanical deformation of the γ phase, would seem to be unlikely if the two phases were composed of chains with the same extended conformation as proposed by Hasegawa et al.[3] However, since it is known that the α phase undergoes a similar transition to the β phase[1,3,4,8] and since the chain conformation of the γ phase can be taken to be a high-energy intermediate between that of the α and β phases, the γ → β transition is quite predictable.

Also, this work poses a question regarding the chain packing in the α and δ (polar α or phase IV) phases of PVF_2. We have shown here that statistical parallel–antiparallel chain packing is present in the γ phase. As the α phase can undergo a solid-state transition to the γ phase, it is possible that statistical parallel–antiparallel packing is also present in the α phase. This possibility is supported by the work of Doll and Lando,[4] who found that two equally likely structures for the α phase could be proposed, one with parallel-chain packing and one with antiparallel packing. Of course, if statistical parallel–antiparallel packing is in fact present in the α phase, one would expect

it to also be present in the δ phase.

Finally, it should be recognized that in this structure there is a clear violation of the equivalency postulate,[28] since the asymmetric unit of structure contains two chemically identical monomer units which have different conformations (TT vs. TG).

Conclusions

The structure of the γ phase of PVF_2 has been determined. The unit cell is orthorhombic with dimensions $a = 0.497$, $b = 0.966$, and $c = 0.918$ nm. The chain conformation is approximately TTTGTTTG'. Individual chains have a net electrical dipole, and the chain packing is such that the unit cell is polar. The chains pack in a statistical parallel–antiparallel manner. The statistical nature of the structure can be modeled with a hypothetical four-chain unit cell belonging to space group $C2cm$. The residuals for this structure are $R' = 0.174$ and $R'' = 0.253$.

Acknowledgment. This research was supported by the Defense Advanced Research Projects Agency and monitored by the Army Night Vision Laboratory under Contract No. DAAK 70-77-C-0055.

References and Notes

(1) J. B. Lando, H. G. Olf, and A. Peterlin, *J. Polym. Sci., Part A-1*, **4**, 941 (1966).
(2) W. M. Prest, Jr., and D. J. Luca, *J. Appl. Phys.*, **46** (10), 4136 (1975).
(3) R. Hasegawa, Y. Takahashi, Y. Chatani, and H. Tadokoro, *Polym. J.*, **3** (5), 600 (1972).
(4) W. W. Doll and J. B. Lando, *J. Macromol. Sci., Phys.*, **B4** (2), 309 (1970).
(5) G. T. Davis, J. E. McKinney, M. G. Broadhurst, and S. C. Roth, *J. Appl. Phys.*, **49** (10), 4998 (1978).
(6) D. Naegele, D. Y. Yoon, and M. G. Broadhurst, *Macromolecules*, **11** (6), 1297 (1978).
(7) G. R. Davies and H. Singh, *Polymer*, **20**, 772 (1979).
(8) R. Hasegawa, M. Kobayashi, and H. Tadokoro, *Polym. J.*, **3** (5), 591 (1972).
(9) W. W. Doll and J. B. Lando, *J. Macromol. Sci., Phys.*, **B2** (2), 219 (1968).
(10) W. M. Prest, Jr., and D. J. Luca, *J. Appl. Phys.*, **49** (10), 5042 (1978).
(11) S. Osaki and Y. Ishida, *J. Polym. Sci., Polym. Phys. Ed.*, **13**, 1071 (1975).
(12) A. J. Lovinger and H. D. Keith, *Macromolecules*, **12** (5), 919 (1979).
(13) G. Cortilli and G. Zerbi, *Spectrochim. Acta, Part A*, **23**, 2216 (1967).
(14) Ye. L. Gal'Perin, B. P. Kosmynin, and R. A. Bychkov, *Vysokomol. Soedin., Ser. B*, **12**, 555 (1970).
(15) M. Kobayashi, K. Tashahiro, and H. Tadokoro, *Macromolecules*, **8**, 158 (1975).
(16) S. Weinhold, M. H. Litt, and J. B. Lando, *J. Polym. Sci., Polym. Lett. Ed.*, **17**, 585 (1979).
(17) M. A. Bachmann, W. L. Gordon, J. L. Koenig, and J. B. Lando, *J. Appl. Phys.*, **50** (10), 6016 (1979).
(18) S. K. Tripathy, R. Potenzone, Jr., A. J. Hopfinger, N. C. Banik, and P. L. Taylor, *Macromolecules*, **12**, 656 (1979).
(19) N. C. Banik, P. L. Taylor, S. K. Tripathy, and A. J. Hopfinger, *Macromolecules*, **12**, 1015 (1979).
(20) M. H. Litt, S. Mitra, and J. B. Lando, to be submitted to *Macromolecules*.
(21) G. J. Welch, *Polymer*, **15**, 429 (1974).
(22) P. J. C. Smith and S. Arnott, *Acta Crystallogr., Sect. A*, **34**, 3 (1978).
(23) "International Tables for X-Ray Crystallography", Vol. 1, Kynoch Press, Birmingham, England, 1952, p 126.
(24) W. W. Doll and J. B. Lando, *J. Macromol. Sci., Phys.*, **B4** (4), 889 (1970).
(25) K. Matsushige and T. Takemura, *J. Polym. Sci., Polym. Phys. Ed.*, **16**, 921 (1978).
(26) K. Matsushige, K. Nagata, and T. Takemura, *Jpn. J. Appl. Phys.*, **17** (3), 467 (1978).
(27) J. Scheinbeim, C. Nakafuku, B. A. Newman, and K. D. Pae, *J. Appl. Phys.*, **50** (6), 4399 (1979).
(28) G. Natta and P. Corradini, *Nuovo Cimento, Suppl.*, **15**, 9 (1960).

The effect of surface nucleation on the crystallization of the α phase of poly(vinylidene fluoride)

S. Weinhold, M. H. Litt, and J. B. Lando
Department of Macromolecular Science, Case Institute of Technology, Case Western Reserve University, Cleveland, Ohio 44106

Transcrystalline films of the α polymorph of poly(vinylidene fluoride) have been prepared. X-ray diffraction shows that such films have a high degree of crystallographic orientation normal to the surface. The orientation shows that the b axis of the α phase unit cell is the principal crystal-growth direction. As is well established for other systems, it was found that the formation and growth of a transcrystalline layer requires relatively dense surface nucleation combined with sparse nucleation in the interior of the film. Experimental variables which favor the formation of surface nuclei include high polymer molecular weight, a mold surface which acts as a nucleating agent (such as Teflon), and a temperature gradient through the film during crystallization. Films exhibiting virtually no nucleation in the interior could be prepared from very pure PVF_2 synthesized in our lab, while samples prepared from biaxially oriented films showed very dense internal nucleation. Annealing at high melt temperatures drastically decreased the internal nucleation in these films. An explanation to account for the behavior is proposed.

PACS numbers: 68.10.Cr, 82.60.Nh, 81.20.Sh

I. INTRODUCTION

It is well known that the surface morphology of many semicrystalline polymers can be substantially different from that present in the bulk. More specifically, while the interior of most semicrystalline polymers is spherulitic, a transcrystalline surface layer is often observed.[1-9] It is generally agreed in the published literature that the transcrystalline layer consists of elongated spherulites which have been nucleated at the surface.

The purpose of this paper is to report a process we have developed for preparing thin transcrystalline films of the α polymorph of poly(vinylidene fluoride), PVF_2. It is a compression molding technique similar to that used by a number of workers investigating the surface crystallization of polymers.[6,7] The effects of several material and processing variables on the morphology of the film are reported. Specifically, the effects of the following variables are discussed: polymer molecular weight, film thickness, processing history of the polymer, type of mold surface, and melt temperature. The effect of a temperature gradient across the film during crystallization was also studied.

This work was undertaken because it may eventually lead to a greater understanding of the origins of the piezoelectric and pyroelectric activity of PVF_2. While PVF_2 has been the subject of intense investigation since it was reported that thin films could exhibit large piezoelectric[10] and pyroelectric[11] coefficients, considerable disagreement still exists concerning the origin of these phenomena. However, it has become increasingly clear that the application of a poling field across the film can cause reorientation of molecular dipoles in the crystal phase.[12-21] It has also been shown that strong poling fields can induce nonpolar α-PVF_2 to convert to polar crystal forms.[12,13,16,21,22-24] Transcrystallization can result in films in which the orientation distribution of polymer dipoles is relatively well defined. We are hopeful that such films may help to shed light on the apparent correlation between dipole orientation and electrical activity, and on the process of dipole reorientation under the influence of a poling field.

II. EXPERIMENTAL

A. Materials

Samples from two sources were employed in this work. The commercially available polymer used was 25-μm-thick Kureha KF biaxially oriented film. By our measurement, the viscosity average molecular weight of this material is 5.15×10^5. Also used were samples of PVF_2 synthesized in our lab. Briefly, the synthesis consists of double distilling vinylidene fluoride gas under vacuum into a Parr stainless-steel pressure and vacuum-tight bomb, where it is subjected to several freeze-degas-melt cycles. The bomb is then placed in a constant-temperature bath and irradiated with ^{60}Co γ radiation which initiates the polymerization. A suitable chain transfer agent, usually n-hexane, may also be added to the bomb before irradiation to control the molecular weight of the resultant polymer. A more detailed description of this synthesis is to appear elsewhere.[25]

Two samples of the lab-synthesized PVF_2, of drastically different molecular weight, were used in this study. Sample HMW, with a viscosity average molecular weight of 7.0×10^6, was polymerized at 0 °C with no chain transfer agent present. Sample LMW, with a viscosity average molecular weight of 2.41×10^5, was polymerized at −43 °C in the presence of 1.2 wt% n-hexane.

Molecular weights were determined from the intrinsic viscosity of the polymer using the relation[26] $[\eta] = 1.93\times10^{-4}M^{0.667}$. Viscosities were measured in N, N-dimethylacetamide (DMAc) solution at 25 °C using an Ubbelohde dilution viscometer. The intrinsic viscosity $[\eta]$ was determined by extrapolating $(\eta_{rel}^{-1})/c$ to $c = 0$. It should be noted that

 0021-8979/80/105145-11$01.10

the molecular weight reported for the HMW material is only approximate, as its viscosity is well outside the limits for which the molecular-weight–viscosity relationship was established.[26]

B. Sample preparation

Sample LMW was used either as synthesized or as a film cast from DMAc solution. Sample HMW was used only in the form of a cast film. As a result of its extremely high molecular weight, this material is quite intractable, and coherent thin films could not be produced by compression molding from the as-synthesized polymer. The Kureha sample was used either as received or as a cast film.

Cast films were produced by dissolving the PVF_2 in DMAc, casting the solution onto clean glass plates using a casting knife, and evaporating the solvent at 90–110 °C. Solutions of the Kureha material contained small fibrous particles which could be removed by centrifugation. To determine whether these particles had any effect on crystallization behavior, films of this polymer were cast from both centrifuged and uncentrifuged solution. Cast films varied in thickness between 10 and 25 μm.

C. Crystallization procedure

A compression molding press manufactured by Pasadena Hydraulics was used to produce the melt-crystallized films. Films of various thicknesses were molded at several temperatures. Films were usually pressed between two pieces of aluminum foil coated with Dupont Teflon. The effect of molding against uncoated aluminum foil, which presumably has an aluminum oxide surface layer, was also determined. The polymer-foil sandwiches are pressed between two plates of $\frac{5}{16}$-in.-thick tool steel.

The films were crystallized either by switching off the press heaters and allowing the unit to cool by natural convection at the rate of approximately 1.5–2.5 °C/min or by creating a temperature gradient across the thickness of the film. The gradient was produced by opening the press to expose the top surface of the upper tool steel plate, placing an aluminum tray containing boiling water onto this surface, and switching off the press heaters. These conditions produced a cooling rate of approximately 2–5 °C/min. Crude calculations show that the magnitude of the gradient produced in this manner is on the order of several hundred ° C/cm.

D. DSC

Differential scanning calorimetry was used to determine the effect of melt temperature on the crystallization temperature of the polymer. Measurements were performed using a Perkin-Elmer DSC-2 equipped with a base-line autozero unit. Temperatures were calibrated with an indium standard.

E. X-ray diffraction

Wide-angle x-ray diffraction was used to determine the degree of preferred crystalline orientation normal to the surface of the sample films. Diffraction patterns were obtained with an evacuated flat-plate x-ray camera using nickel-filtered Cu$K\alpha$ radiation.

To minimize exposure time, x-ray samples were prepared by gluing several pieces of film together with rubber cement. The samples were positioned such that the direction of the x-ray beam was parallel to the surface of the film.

F. Optical microscopy

Microscopy samples were sectioned from the PVF_2 films with a Reichert microtome and mounted between a glass slide and cover slip. Optical micrographs were taken with the sample between crossed polarizers on a Zeiss microscope equipped with a 35-mm camera.

III. MODEL FOR TRANSCRYSTALLIZATION

As an aid to interpreting the results presented below, it is appropriate at his point to review in a general manner the processes which occur during the nucleation and growth of a transcrystalline layer. To this end, a model of the sequence of events producing a transcrystalline layer is presented. The initial form is very simplistic but accounts for the essential processes involved; it is subsequently modified to be more complex and realistic. The concepts discussed in the model are not new and are generally well accepted.

Consider a polymer melt at a temperature above the melting point of the polymer in contact with a surface, and extending to infinity away from the surface. The melt is completely homogeneous and free from impurities. The temperature of this system is then decreased infinitely quickly and maintained at a point below T_m. However, the undercooling is not sufficiently great to allow true homogeneous nucleation. The surface has the ability to stabilize small aggregations of polymer chains (primary nuclei) which are in contact with it. Stabilization is achieved by decreasing the surface free energy of a small nucleus, thereby reducing the critical size required for stability. For convenience sake, the ability of the surface to stabilize small nuclei will be called nucleating ability. Different surfaces may possess different degrees of nucleating ability.

After the temperature is lowered, stable primary nuclei form at the surface. The average distance between such nuclei is d. Crystal growth then proceeds from the surface nuclei. The growth is hemispherulitic; that is, lamella grow in all possible directions into the melt. Growth proceeds in this manner until the average hemispherulite diameter is equal to d. At this point neighboring hemispherulites are just beginning to impinge. Since lamellar growth has been equally likely in all possible directions, no preferred lamellar (and hence crystallographic) orientation exists. After impingement, lamella can no longer grow parallel to the surface. Growth can occur only in directions with a component normal to the surface. As the distance l between the crystal-growth front and the surface increases, lamellar growth can occur only in directions with an increasingly greater component normal to the surface. As the ratio l/d becomes large, individual hemispherulites become more or less cylinderical in shape, with a diameter d and length l. At large l/d, the lamellar orientation distribution is much greater in the direction normal to

the surface than parallel to the surface. Thus, lamellar orientation exists such that the lamellar-growth direction is preferentially oriented normal to the surface. The degree of preferred orientation can be quantitatively determined using either wide- or small-angle x-ray diffraction. The degree of preferred orientation is thus an indirect measure of l/d. This oriented surface layer is commonly called a transcrystalline layer. Of course, for an infinitely thick film, $l/d \rightarrow \infty$ as the crystallization time approaches infinity.

A more reasonable transcrystalline model is that of a film of finite thickness. For this the above model is modified such that the melt is bounded by a second surface which has no nucleating ability and which is situated parallel to the first surface at a distance t away from it. The the thickness of the transcrystalline layer grown from this sytem is equal to t and $l/d = t/d$. If the density of surface nuclei is such that

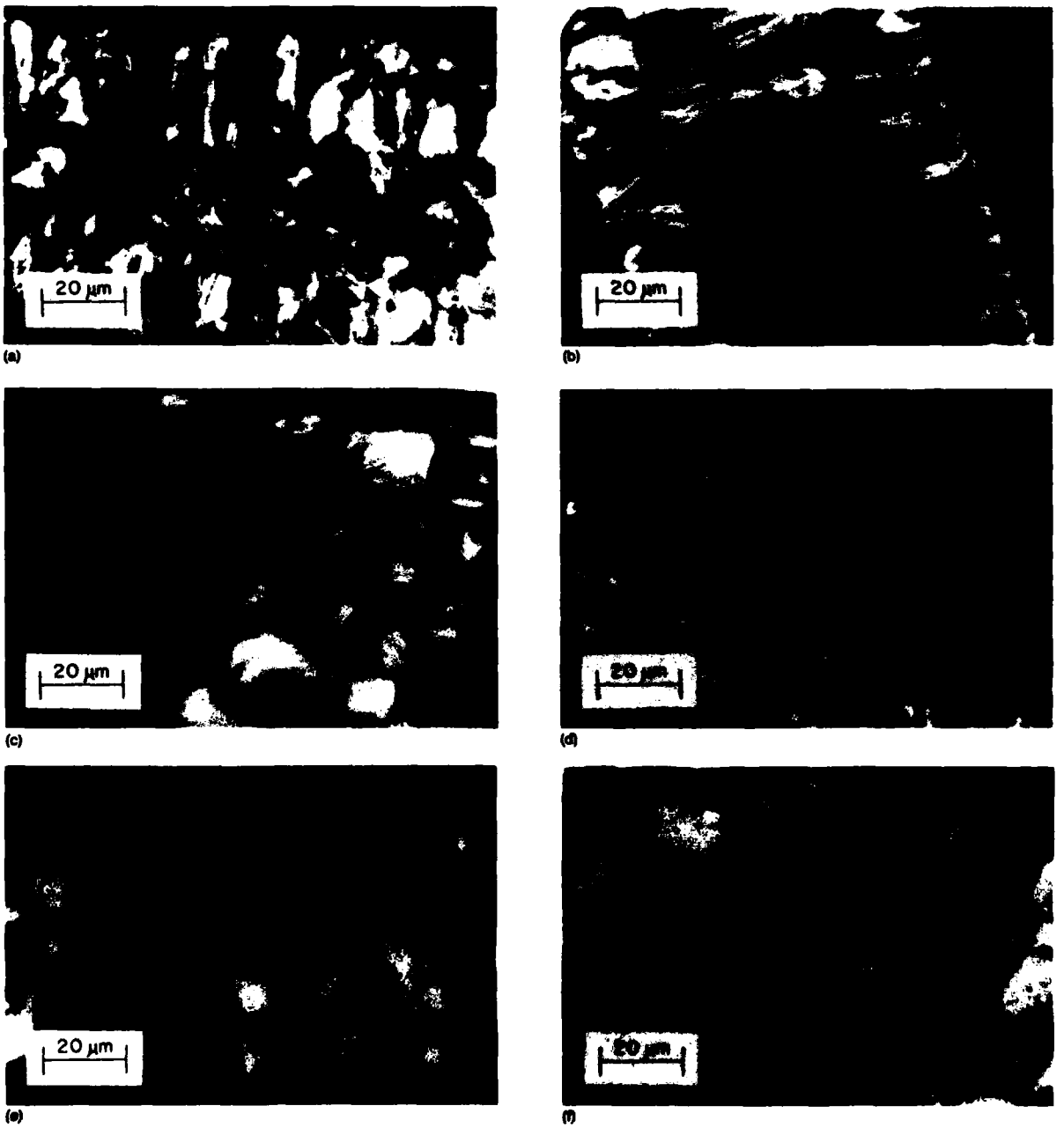

FIG. 1. Optical micrographs of microtome sections of PVF_2 films. All films were molded between Teflon surfaces at 200 °C and crystallized with a temperature gradient through the film unless otherwise noted. Films were molded from (a) LMW cast film; (b) LMW as-synthesized material; (c) Kureha film as received; (d) Kureha film cast from DMAc; (e) Kureha film as received, molded at 245 °C; (f) Kureha film as received, molded at 245 °C with aluminum foil as the warmer mold surface.

$d \approx t$, no preferred lamellar orientation exists. To achieve some degree of preferred orientation, it is necessary to either increase t or decrease d. The latter option, increasing the density of surface nuclei, can be accomplished in three ways:

(1) Decrease the temperature of the nucleating surface. This has the effect of decreasing the critical size for a stable nucleus.

(2) Modify the physical and/or chemical nature of the surface to increase its ability to stablize nuclei.

(3) Modify the polymer to enhance its ability to form primary nuclei at the surface. This condition can be met by increasing its molecular weight.

If the inert surface in the model above is replaced by a surface with some nucleating ability, nucleation sites will be present at both surfaces and $l_{max} = \frac{1}{2}t$.

Changing the model once again to be more realistic, assume that heterogeneous nuclei are dispersed throughout the film. For the present, we define heterogeneous nuclei as

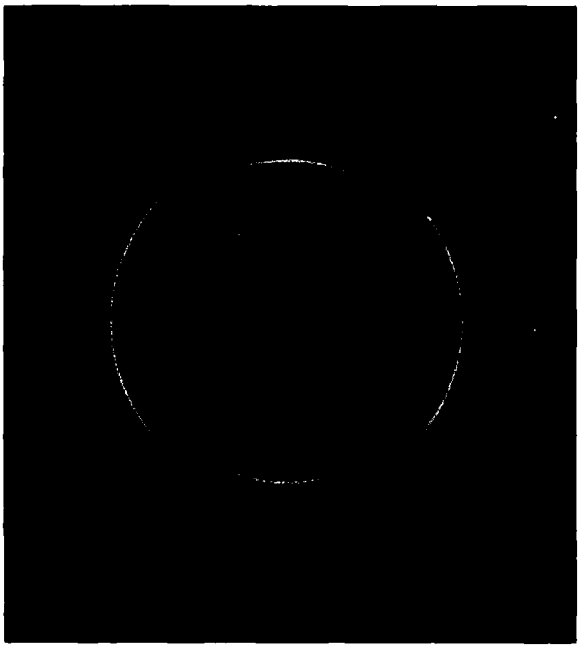

(a)

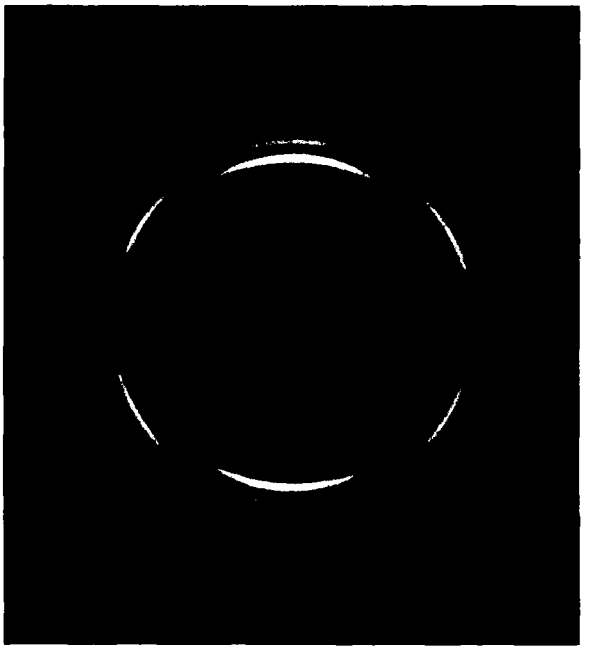

(b)

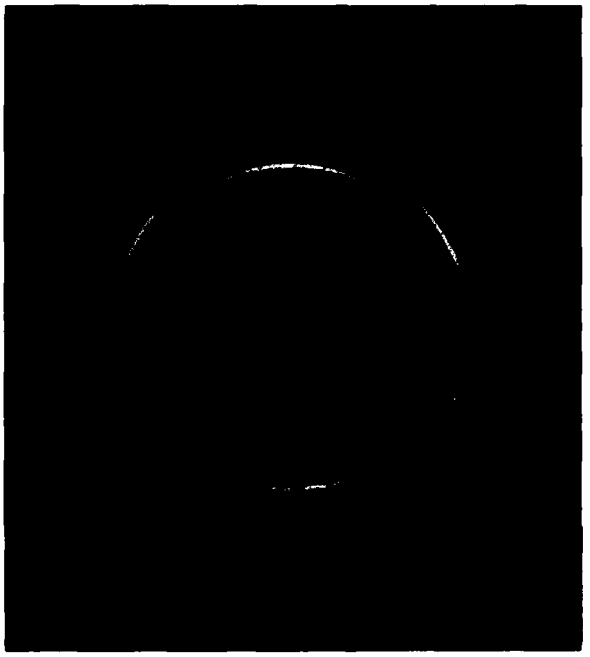

(c)

FIG. 2. Diffraction photographs of PVF_2 films. The photographs were taken with the normal of the sample film vertical. All films were molded between Teflon surfaces at 200 °C and crystallized with a temperature gradient through the film unless otherwise noted. Films were molded from (a) LMW cast film, shows moderate orientation; (b) HMW cast film molded at 214 °C, shows very high orientation; (c) LMW as-synthesized material, shows very high orientation.

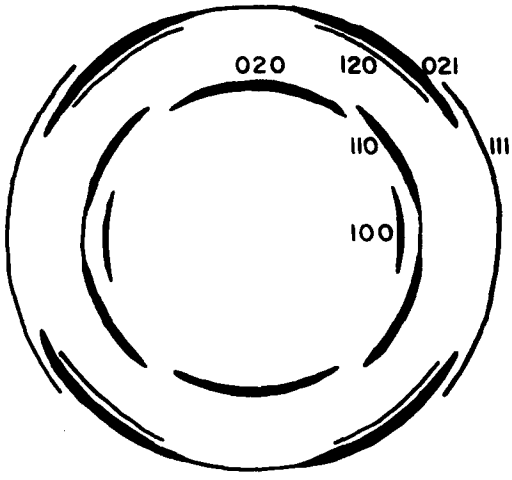

FIG. 3. Drawing of a typical diffraction pattern showing the indices of the reflections.

small particles which differ in some physical and/or chemical manner from the surrounding polymer melt, and which possess a certain nucleating ability for exactly the same reasons as nucleating surfaces. If the nucleating ability of the hetergeneous nuclei is greater than that of the surfaces, little surface nucleation will occur and the morphology of the crystallized film will be spherulitic, with the size of the spherulites inversely proportional to the density of heterogeneous nucleation. If the surfaces have a greater nucleating ability than the heterogeneous nuclei, surface nucleation and transcrystalline growth will proceed unhindered.

Let us now consider nonisothermal conditions such that the temperature decreases with time uniformly throughout the film. If the nucleating ability of the heterogeneous nuclei is greater than that of the surfaces, the result is identical to that of the isothermal case and the film will be entirely spherulitic. If the nucleating ability of the surfaces is greater than that of the heterogeneous nuclei, surface nucleation and transcrystalline growth from both surfaces will occur. However, as the temperature decreases, the activity of the heterogeneous nuclei increases.

Heterogeneous nucleation and spherulitic growth can then occur if the interior of the film has not yet been incorporated into the advancing transcrystalline layers. Whether or not this will occur is dependent upon the relative nucleating ability of the heterogeneous nuclei and the surfaces, the rate of temperature decrease, and the lamellar growth rate of the polymer.

As a final complexity, assume that, as well as nonisothermal conditions, the temperature profile through the thickness of the film is nonuniform such that a linear temperature gradient exists through the film. As the temperature decreases, nucleation followed by crystal growth will occur. The location and extent of nucleation is dependent on the nucleating ability of the surfaces relative to that of the heterogeneous nuclei, the steepness of the temperature gradient, the rate of temperature decreases, and the lamellar growth rate. The result can be completely transcrystalline film nucleated at one or both surfaces, a completely spherulitic film, or a film with a transcrystalline layer at one or both surfaces with spherulites occupying the remainder of the film. Spherulites occupying a portion of the film decreases l_{max} and hence decreases the maximum degree of preferred orientation achievable. Internal heterogeneous nucleation is minimized by employing a steep temperature gradient and decreasing the temperature slowly. Of course, the removal or deactivation of the heterogeneous nuclei would also eliminate spherulitic growth.

Many of the general concepts and conclusions of this model will be demonstrated below with specific examples.

IV. RESULTS AND DISCUSSION

Figure 1 shows optical micrographs of several compression-molded PVF_2 films. Figure 2 shows the x-ray diffraction patterns of some of these samples. Also shown in Fig. 2 is the diffraction patterns of a molded HMW cast film. No micrographs of HMW films are shown because no morphological structure could be resolved with the optical microscope. The degree of preferred crystalline orientation normal to the surface of these films is determined from the angle subtended by a given spot on the diffraction pattern, i.e., the smaller the subtended angle, the greater the degree of preferred orientation. Figure 3 shows a sketch of a typical diffraction pattern with the spots indexed on the basis of the well-established structure of α-PVF_2.[27,28]

X-ray diffraction showed that all compression-molded samples contained only the α crystal form. Also, it is evident from the diffraction patterns that the b axis of the α unit cell is oriented normal to the surface. This observation indicates that the b axis is the dominant crystal-growth direction in α-PVF_2, in agreement with the results of Lovinger and Wang.[29]

The dependence of morphology and degree of preferred orientation on polymer molecular weight, film thickness, processing history, molding temperature, and mold surface are reported below. Also discussed is the effect of a temperature gradient during crystallization. All specimens were held at the peak melt temperature for 5–10 min. Varying the time between these limits while holding all other parameters constant had no detectable effect. Also, varying the peak melt temperature between 200 and 214 °C had no observable effect for any material. Finally, all films were molded between two Teflon surfaces unless otherwise noted.

A. Polymer molecular weight

Table I shows the effect of molecular weight on the density of surface nucleation. All specimens were molded from cast films and crystallized in the presence of a temperature gradient. Specimen 2 possess a very high degree of preferred orientation, showing that l/d is large. Specimen 1 possesses only a very low degree of preferred orientation. Since the film thickness t (and subsequently l) is essentially the same for both specimens, this shows that d is much smaller in the high-molecular-weight specimen than in the low-molecular-weight sample, i.e., the density of surface nuclei is much greater.

TABLE I. The effect of molecular weight on degree of preferred orientation.

Specimen number	Material	Melt temperature (°C)	Film thickness (μm)	Degree of preferred orientation
1	LMW, cast	200	18	Very low
2	HMW, cast	214	20	Very high Fig. 2(b)

We interpret these results in the following manner. First, Teflon has the ability to nucleate the crystallization of α-PVF_2 under these conditions. This was not a completely unexpected result in that it has been shown that Teflon can nucleate the crystallization of both isotactic polypropylene[7] and polyethylene.[30] Second, we believe that the smaller d of the HMW specimen is a result of very-high-molecular-weight molecules adsorbing onto the surface much more readily than lower-molecular-weight chains. This belief is based on the knowledge that during crystallization from dilute solutions, high-molecular-weight polymer molecules are the first to crystallize, and thus serve as crystallization nuclei.[31,32] Also, during epitaxial crystallization from dilute solution, it has been shown[33,34] that high-molecular-weight polymer is adsorbed onto the substrate surface much more readily than lower-molecular-weight material.

This conclusion was reached after considering the effects that melt orientation might have surface nucleation. It is probable that some amount of chain orientation is introduced into the melt by the forces encountered during molding. This orientation would be such that the PVF_2 chains lie in the plane of the films, almost certainly a favorable orientation for the formation of surface nuclei. The time necessary for the relaxation of the melt orientation would be much longer for the HMW material than for the LMW polymer. Thus, at the time of crystallization, significant orientation could remain in the HMW melt, while all orientation may have disappeared from the LMW melt. Increasing the melt temperature would decrease the relaxation time, and if melt orientation plays a role in surface nucleation, it could decrease the density of surface nuclei.

Table II shows the effect of raising the melt temperature from 214 (specimen 2) to 245 °C (specimen 3). Indeed, increasing the melt temperature does decrease the degree of preferred orientation somewhat. However, increasing the melt temperature decreases the melt viscosity so that greater flow occurs in response to compression, resulting in a thinner film. Thus, the smaller t of specimen 3 may contribute to the decrease in orientation. On the other hand, specimen 4 shows that orientation of the melt is certainly not a prerequsite for the formation of surface nuclei. Specimen 4 was prepared by placing a piece of HMW cast film, which was crystallographically isotropic as measured by x-ray diffraction, on a Teflon surface, heating to 218 °C in an oven, and lowering the temperature at about 1.5 °C/min. No orientation of the melt is produced by such a procedure. The moderate degree of preferred orientation demonstrates the presence of a substantial density of surface nuclei. Had speciment 4 been crystallized in a temperature gradient, the degree of preferred orientation would be expected to be even greater. The effect of a temperature gradient is discussed in greater detail later.

B. Film thickness

Table III illustrates the effect of film thickness on the degree of preferred orientation achievable under a given set of conditions. Specimens 1 and 5 were both molded at 200 °C from cast LMW film and crystallized in a temperature gradient. The substantially greater orientation in the thicker film is simply due to a greater l/d ratio than in the thinner film.

Figure 1a shows a section of the thicker film. For the thicker transcrystalline layer (which was nucleated at the colder surface), d is on the order of 10μm and l is approximately 40μm, so that $l/d \approx 4$. A relatively high degree of orientation is expected in a layer with such a ratio; however, the spherulitic interior and transcrystalline layer originating from the warmer surface (where l/d is small) decrease the average orientation in the film as a whole. For the thinner film, if one assumes that d remains unchanged, that $l = \frac{1}{2}t$ for both layers (a reasonable assumption, as a small t means that the difference in temperature between the two surfaces is small, so that nucleation will occur at both surfaces at about the same time), and that the film has no spherulitic interior, the characteristic ratio $l/t \approx 1$. Thus, little or no orientation is expected.

TABLE II. The effect of melt temperature and compression of the melt on the degree of preferred orientation of HMW material.

Specimen number	Melt temperature (°C)	Film thickness (μm)	Temperature gradient during crystallization?	Compression molded?	Degree of preferred orientation
2	214	20	Yes	Yes	Very high Fig. 2(b)
3	245	15	Yes	Yes	High
4	218	25	No	No	Moderate

TABLE III. The effect of film thickness on the degree of preferred oreintation.

Specimen number	Film thickness (μm)	Morphology*	Degree of preferred orientation
1	18	...	Very low
5	85	Transcrystalline surface layers, spherulitic interior Fig. 1(a)	Moderate Fig. 2(a)

* A dash indicates that there was no direct observation of morphology.

As well as the specimens shown in Table III, a number of films of intermediate thicknesses were molded from cast LMW and cast Kureha films. A strong correlation between film thickness and degree of orientation was found for all of these films.

C. Processing history

The morphology resulting from crystallization under a given set of conditions is strongly dependent on the processing history of the material. This is illustrated in Table IV. All specimens were molded at 200 °C and crystallized in a temperature gradient.

Specimen 6 was molded from LMW polymer taken directly from the reaction bomb. Thus, there was little opportunity to contaminate the polymer with foreign material. Figure 1b shows that the morphology of the film is completely transcrystalline. When the same material was dissolved and cast prior to molding [specimen 5, Fig. 1(a)], the central portion of the film was spherulitic. The spherulites show that some sort of crystallization nuclei had been introduced during the casting process. These nuclei may consist of either small particles of foreign matter or small domains of polymer in which some remnant of crystalline order remains. However, as is discussed in greater detail later, the internal nuclei in cast films are insensitive to melt temperature, which suggests that the nuclei are foreign.

Specimen 7, molded from cast Kureha material and shown in Fig. 1(c), has a morphology very similar to that of specimen 5. Specimen 7 was molded from a film cast from a centrifuged solution. Similar films made from uncentrifuged solutions showed the same degree of orientation. Thus, the numerous small fibers observed in uncentrifuged solutions of the Kureha material either (1) do not act as crystallization nuclei or (2) are effective nuclei, but are too few in number to significantly alter the overall morphology of the film.

Specimen 8 was molded from as-received Kureha film. Figure 1(d) shows that this film is composed entirely of small spherulites; no transcrystalline surface layers are present. Such a morphology requires that a large number of very efficient crystallization nuclei are present in the melt. There appears to be a monotonic change in the average sperulite diameter through the thickness of the film. Fitchmun and Newman[7] have reported a similar observation for isotactic polypropylene compression molded against aluminum oxide and rapidly crystallized in a temperature gradient. They found the smallest spherulites were closest to the relatively cold surface, with the average spherulite size increasing with distance from the surface. Therefore, we assume that the temperature gradient is responsible for the spherulite-size distribution observed in this film.

It is apparent that the solution casting process in some manner deactivates the vast majority of the crystallization nuclei in the as-received Kureha film. It is shown below that a high melt temperature has the same effect.

TABLE IV. The effect of processing history on morphology and degree of preferred orientation.

Specimen number	Material	Film thickness (μm)	Processing history	Morphology	Degree of preferred orientation
5	LMW	85	Cast	Transcrystalline surface layers, spherulitic interior; Fig. 1(a)	Moderate, Fig. 2(a)
6	LMW	90	As-synthesized	Completely transcrystalline, Fig. 1(b)	Very high, Fig. 2(c)
7	Kureha	118	Cast	Transcrystalline surface layers, spherulitic interior; Fig. 1(c)	Moderate
8	Kureha	88	As-received	Small spherulites throughout, Fig. 1(d)	None

TABLE V. The effect of melt temperature on the morphology and degree of preferred orientation of as-received Kureha film.

Specimen number	Film thickness (μm)	Melt temperature (°C)	Morphology	Degree of preferred orientation
8	88	200	Small spherulites throughout, Fig. 1(d)	None
9	80	214	Small spherulites throughout	None
10	65	245	Transcrystalline surface layers, spherulitic interior; Fig. 1(e)	Moderate

D. Molding temperature

Table V shows the effect of melt temperature on films molded from as-received Kureha material and crystallized in a temperature gradient. At some temperature between 214 and 245 °C, the vast majority of crystallization nuclei become deactivated. Similar relations between nucleation density and melt temperature have been observed for polyethylene[35] poly (ethylene oxide)[36] isostatic polypropylene,[37] and other polymers.[38] Only the as-received Kureha material showed this marked dependence of morphology on melt temperature.

Several investigators have used DTA to study the effect which heterogeneous nucleating agents had on the crystallization temperature.[39-41] It was found that the addition of effective nucleating agents considerably increased the crystallization temperature. We have used DSC in a similar manner, but with the goal of detecting a decrease in the crystallization temperature due to the deactivation of crystallization nuclei.

Four samples were investigated by DSC. They were as-received and cast Kureha film, and as-synthesized and cast LMW material. Samples weighing about 3.5 mg were heated to 210 °C, held at that temperature for 3–5 min, then cooled to 100 °C; this cycle was then repeated. It was followed by a cycle to 250 °C, and finally followed by another cycle to 210 °C. All heating and cooling rates were 20 °C/min. The melting temperature of all specimens, defined here as the temperature of the peak of the melting endotherm, was between 174 and 177 °C. Additional results are shown in Table VI. $T_{c\,210}$ is the crystallization temperature after the initial heating to 210 °C. $T_{c\,250}$ is the crystallization temperature after heating to 250 °C. In this case, the crystallization temperature is defined as the temperature at which the crystallization exotherm first deviates from the base line. This is the temperature at which large-scale crystallization begins.

In all cases, the crystallization temperature after the second heating to 210 °C was not significantly different from the crystallization temperature after the initial heating to 210 °C. The effect of heating to 250 °C varied from sample to sample. Little change in crystallization temperature was observed for the as-synthesized LMW material and for both cast samples. A relatively large decrease in the crystallization temperature was noted for the as-received Kureha film. Also, this decrease in T_c was permanent in the sense that little increase in the crystallization temperature was noted after a subsequent cycle to 210 °C. These results confirm that the numerous nuclei in the Kureha film are deactivated by high melt temperatures. Also, the similar value of $T_{c\,250}$ for the as-received and cast Kureha films confirm that the casting process also deactivates these nuclei. Furthermore, it is apparent that once these nuclei are deactivated, they are not regenerated by subsequent crystallization.

E. Mold surface

It has been shown above that Teflon has the ability to nucleate a transcrystalline layer if the PVF_2 melt is not contaminated with numerous highly active crystallization nuclei. Table VII shows that the nucleating ability of aluminum oxide is substantially less than that of Teflon. All films were crystallized in a temperature gradient. Specimen 10, molded between two Teflon surfaces, has transcrystalline layers originating from both surfaces [Fig. 1(e)]. Specimen 11, molded between one Teflon and one aluminum oxide surface, has only a single transcrystalline layer [Fig. 1(f)]. Thus, it is evident that aluminum oxide has very little ability to nucleate the crystallization of Kureha PVF_2 under these conditions.

On the other hand, it is also clear that aluminum oxide

TABLE VI. The dependence of crystallization temperature on melt temperature.

	Kureha as-received	Kureha cast	LMW as-synthesized	LMW cast
$T_{c\,210}$ (°C)	149	145	143	150
$T_{c\,250}$ (°C)	145	144	144	149

TABLE VII. The effect of the nature of the mold surface on surface nucleation and morphology.

Specimen number	Material	Film thickness (μm)	Melt temperature (°C)	Mold surface: Warmer surface	Mold surface: Colder surface	Morphology: Warmer surface	Morphology: Colder surface	Degree of preferred orientation
10	Kureha as-received	65	245	Teflon	Teflon	Transcrystalline Fig. 1(e)	Transcrystalline	Moderate
11	Kureha as-received	65	245	Al_2O_3	Teflon	Spherulitic Fig. 1(f)	Transcrystalline	Moderate
2	HMW, cast	20	214	Teflon	Teflon	...	...	Very high, Fig. 1(b)
12	HMW, cast	20	200	Al_2O_3	Al_2O_3	...	...	High

can promote the nucleation of HMW material quite readily, although not as well as Teflon does. We can offer no real explanation for the relative nucleating ability of Teflon as compared to aluminum oxide since we know of no theory which adequately explains why some materials are effective nucleating for a given polymer melt while other materials are not.

F. Temperature gradient

When a temperature gradient is created across the thickness of a molten film of PVF_2, the melt adjacent to the mold surface is at a lower temperature than the melt in the interior of the film. Thus, if the mold surface is at all capable of nucleating the crystallization of PVF_2, the presence of a temperature gradient enhances the relative nucleating ability of the surface with respect to that of nuclei dispersed throughout the film. Such a condition favors the formation of a transcrystalline layer. However, it is generally agreed that a surface with sufficiently great nucleating ability can nucleate a transcrystalline layer even in the absence of a temperature gradient.[5,7,9]

Table VIII compares the degree of preferred orientation of similar films crystallized in a temperature gradient and in the absence of a gradient. All specimens were molded between Teflon. A substantial degree of orientation is present in both HMW and LMW films crystallized without a gradient, but crystallization in a gradient increases the orientation significantly. Thus, a temperature gradient increases the density of nuclei at the surface, but it is not an essential requirement for the formation of a transcrystalline surface layer.

A few experiments were also done in which the temperature gradient was created by running cold water through a heat exchanger in one of the press platens. This results in a substantially steeper temperature gradient as well as greatly increasing the rate of temperature decrease. Films of Kureha material crystallized in such a manner had a significantly greater degree of orientation than similar films crystallized in a standard temperature gradient.

G. Comments on the nature of the internal nuclei

It is generally agreed that in a slowly cooled fully relaxed polymer melt, homogeneous nucleation occurs only in the complete absence of foreign material which can nucleate crystallization hetergeneously. When very dense nucleation is observed, as in the specimens molded at 200 °C from as-received Kureha film, it must be concluded that either large quantities of foreign contaminants are present or that the melt is not fully relaxed and homogeneous. The fact that the vast majority of nuclei in the Kureha material are destroyed by high melt temperatures strongly suggests that some remnants of molecular order remain in the melt after heating to 200–214 °C for 10 min. This order is destroyed by heating to higher temperatures.

TABLE VIII. The effect of a temperature gradient during crystallization on the degree of preferred orientation.

Specimen number	Material	Melt temperature (°C)	Film thickness (μm)	Temperature gradient during crystallization?	Degree of preferred orientation
2	HMW, cast	214	20	Yes	Very high
13	HMW, cast	214	15	No	Moderate-good
6	LMW, as-synthesized	200	90	Yes	Very high
14	LMW, as-synthesized	200	87	No	Moderate-good

It is necessary to consider the manner in which this film is produced in order to understand the nature of the ordered domains which we feel must exist in the Kureha material up to temperatures of at least 214 °C. As this film is biaxially oriented, it was probably manufactured by an extrusion-blowing technique. Whatever its means of manufacture, the film has undergone large elongational stresses during crystallization. One result of this deformation is that both the α and β crystal forms are present in the film; this has been determined by x-ray diffraciton. Another possible consequence is the formation of columnar crystals with a core of extended high-molecular-weight polymer chains. While we have no direct evidence for this, we believe that such crystals exist in the as-received Kureha film. It is well known that cores of the familiar "shish-kebab" structures, first described by Pennings and Kiel,[42] contain extended-chain polymer. These structures result when extensional flow is present in dilute polymer solutions during crystallization. Similar extended chain cores are known to be formed when polymer melts are subjected to elongational forces during crystallization, resulting in "row structure."[43,44] The extended-chain crystals have a higher melting temperature than chain folded crystals.

While we measure the DSC melting temperature of the as-received Kureha film to be 174 °C and observe no higher temperature transition by DSC, this does not rule out the possible existence of a small quantity of such extended-chain crystals. The DSC experiment is not sensitive enough to detect the melting of a small quantity of such material. If such crystals exist they would probably be in the β crystal phase,[28,45] in which the chain backbone conformation is all *trans* and is thus as extended as much as possible. The melting point of the β phase is higher than that of the α phase, and the melting temperature of relatively large extended-chain β-phase crystals, produced by crystallization under high pressure, has been determined to be 207 °C.[46] This can be considered to be the upper limit for the melting temperature of any extended-chain crystals in the as-received Kureha film.

Since we have shown that profuse nucleation occurs in as-received Kureha film even after heating to 214 °C, it seems very unlikely that extended-chain crystals, as such, are directly responsible for the nucleation. However, the macroconformation of the polymer chains in the crystalline state is to some extent retained even after all true crystalline order has been destroyed (melting has occurred). The rate at which this crystallinelike macroconformation is reduced to a random coil conformation depends on kinetic factors such as temperature and molecular weight. Since the extended-chain crystals are of very-high-molecular-weight material, the rate of decay of conformational order is quite slow at temperatures up to at least 214 °C. Thus, a substantial degree of order is still present when the temperature of the melt has decreased to the point where crystallization can occur. The semiordered chains can then crystallize at a temperature well above that at which the bulk of the melt can crystallize. The resulting crystalline inclusions serve to nucleate the crystallization of the remainder of the melt. When the melt temperature is increased to 245–250 °C, the destruction of conformational order proceeds at a much faster rate than at the lower melt temperatures such that no significant order remains when the temperature is lowered and no early crystallization occurs.

It is evident that disolution in DMAc also destroys the extended-chain crystals. Upon subsequent crystallization from the solution it is probable that the high-molecular-weight component is the first to crystallize, and thus serves to nucleate the crystallization of the remainder of the polymer. Hence, it might be expected that these high-molecular-weight nuclei would behave similarly to those in the as-received Kuerha film. However, since neither the nucleation density nor the crystallization temperature of the cast films is a function of peak melt temperature (within the range considered here), this obviously is not the case. It seems probable that the extended-chain nature of the nuclei in the as-received Kureha film is responsible for the persistance of these nuclei at relatively low melt temperatures.

H. Possible applications

The product obtained from the directional crystallization experiments, i.e., films of α-PVF_2 with relatively-well-defined polymer dipole orientation, may be useful for studying the process of dipole reorientation under the influence of an electric field. Because the polymer dipoles are oriented parallel to the surface of the film ($\pm \sim 30°$ for the most highly oriented films) and because a poling field would tend to align the dipoles as nearly perpendicular to the surface as possible, it may be possible to induce and quantitatively measure a dipole reorientation of less than the 180° rotation which produces the δ (polar α) phase of PVF_2. Some evidence for chain rotation through an angle other than 180° when poling α-PVF_2 has been reported,[12,23,24] but the results are not clear.

Also, the insights and understanding gained through this work may be applied towards the preparation of directionally crystallized β-PVF_2. While it is very unlikely that transcrystalline films of β-phase material could ever be prepared from pure PVF_2,[29] copolymers with vinyl fluoride, tetrafluoroethylene, or trifluoroethylene could be used. These copolymers crystallize into the β phase under ordinary crystallization conditions.[47] Using such materials, it may be possible to prepare a transcrystalline film in the β phase in which all of the polymer dipoles have a unipolar orientation. Dense nucleation at only one surface could produce such films. If the direction of dipole orientation had a component normal to the surface, such films should be pyroelectrically and piezoelectrically active without being subjected to a poling field.

V. CONCLUSIONS

Films of α-PVF_2 with a transcrystalline morphology have been produced. X-ray diffraction patterns of such films show that the *b* axis of the unit cell is the dominant crystal-growth direction of α-PVF_2. The formation of a transcrystalline layer is favored by dense surface nucleation, while nucleation in the interior of the film leads to spherulites

which interfere with the growth of the transcrystalline layer. Experimental variables which promote the formation of surface nuclei include high polymer molecular weight, a mold surface such as Teflon which acts as a nucleating agent, and a temperature gradient through the film during crystallization. Very little internal nucleation occurs in ultrapure PVF_2 synthesized in our lab. Very dense internal nucleation occurs in Kureha biaxially oriented film. These nuclei are deactivated by high melt temperatures or dissolution in DMAc. We propose that these destructable nuclei consist of extended chains of high-molecular-weight polymer derived from extended-chain crystals in which the macroconformation of the chain in the crystalline state persists for long periods of time at relatively low melt temperatures. With the understanding gained through this work, it may eventually prove possible to prepare transcrystalline films of PVF_2 in a polar phase.

ACKNOWLEDGMENTS

This research was supported by the Defense Advanced Research Project Agency and monitored by the Army Night Vision Laboratory under Contract No. DAAK 70-77-C-0055.

[1]E. Jenckel, E. Teege, and W. Hinricks, Kolloid Z. **129**, 19 (1952).
[2]R. J. Barriault and L. F. Gronholz, J. Polym. Sci. **18**, 393 (1955).
[3]R. K. Eby, J. Appl. Phys. **35**, 2722 (1964).
[4]B. B. Burnett and W. F. McDevit, J. Polym. Sci. **20**, 211 (1956).
[5]H. Schonhorn, Macromolecules **1**, 145 (1968).
[6]D. Fitchmun and S. Newman, J. Polym. Sci., Polym. Lett. Ed. **7**, 301 (1969).
[7]D. R. Fitchmun and S. Newman, J. Polym. Sci. A2 **8**, 1545 (1970).
[8]M. R. Kantz and R. D. Corneliussen, J. Polym. Sci., Polym. Lett. Ed. **11**, 279 (1973).
[9]J. R. Shaner and R. D. Corneliussen, J. Polym. Sci. A2 **10**, 1611 (1972).
[10]H. Kawai, Jpn. J. Appl. Phys. **8**, 975 (1969).
[11]J. G. Bergman, Jr., J. H. McFee, and G. R. Crane, Appl. Phys. Lett. **18**, 203 (1971).
[12]G. T. Davis, J. E. Mckinney, M. G. Broadhurst, and S. C. Roth, J. Appl. Phys. **49**, 4998 (1978).
[13]P. D. Southgate, Appl. Phys. Lett. **28**, 250 (1976).
[14]M. Tamura, S. Hagiwara, S. Matsumoto, and N. Ono, J. Appl. Phys. **48**, 513 (1977).
[15]J. P. Luongo, J. Polym. Sci. A2 **10**, 1119 (1972).
[16]D. Naegele, D. Y. Yoon, and M. G. Broadhurst, Macromolecules **11**, 1297 (1978).
[17]E. Fukada, M. Date, and T. Furukawa, Organic Coating Plast. Chem. **38**, 262 (1978).
[18]M. Latour, Polymer **18**, 278 (1977).
[19]D. N. Naegle and D. Y. Yoon, Appl. Phys. Lett. **33**, 132 (1978).
[20]R. G. Kepler and R. A. Anderson, J. Appl. Phys. **49**, 1232 (1978).
[21]D. K. Das Gupta and K. Doughty, Appl. Phys. Lett. **31**, 585 (1977).
[22]D. K. Das Gupta and K. Doughty, J. Phys. D **11**, 2415 (1978).
[23]G. R. Davies and H. Singh, Polymer **20**, 772 (1979).
[24]M. Bachmann, W. L. Gordon, S. Weinhold, and J. B. Lando (unpublished).
[25]M. H. Litt, S. Mitra, and J. B. Lando (unpublished).
[26]G. J. Welch, Polymer **15**, 429 (1974).
[27]W. W. Doll and J. B. Lando, J. Macromol. Sci.–Phys. B **4**, 309 (1970).
[28]R. Hasegawa, Y. Takahashi, Y. Chatani, and H. Tadokoro, Polymer J. **3**, 600 (1972).
[29]A. J. Lovinger and T. T. Wang, Polymer **20**, 725 (1979).
[30]A. G. M. Last, J. Polym. Sci. **39**, 543 (1959).
[31]A. Keller and F. M. Willmouth, J. Polym. Sci. A2 **8**, 1443 (1970).
[32]A. Keller and D. M. Dadler, J. Polym. Sci. A2 **8**, 1457 (1970).
[33]S. H. Carr, A. Keller, and E. Baer, J. Polym. Sci. A2 **8**, 1467 (1970).
[34]S. Wellinghoff, F. Rybuikar, and E. Baer, J. Macromol. Sci.–Phys. B **10**, 1 (1974).
[35]J. Rabesiaka and A. J. Kovacs, J. Appl. Phys. **32**, 2314 (1961).
[36]W. Banks and A. Sharples, Makromol. Chem. **67**, 42 (1963).
[37]J. R. Collier and L. M. Neal, Polymer. Sci. Eng. **9**, 182 (1969).
[38]B. Wunderlich, *Macromolecular Physics* (Academic, New York, 1976), Vol 2, p. 53.
[39]H. N. Beck and H. D. Ledbetter, J. Appl. Polym. Sci. **9**, 2131 (1965).
[40]H. N. Beck, J. Appl. Polym. Sci. **11**, 673 (1967).
[41]A. Yun and L. E. St. Pierre, J. Polym. Sci. B **8**, 241 (1970).
[42]A. J. Pennings and A. M. Kiel, *Kolloid Z.* **205**, 160 (1965).
[43]A. Keller and M. J. Machin, J. Macromol. Sci. Phys. B **1**, 41 (1967).
[44]M. J. Hill and A. Keller, J. Macromol. Sci., Phys. B **3**, 153 (1969).
[45]J. B. Lando, H. G. Olf, and A. Peterlin, J. Polym. Sci. A1 **4**, 941 (1966).
[46]K. Matsushige and T. Takemura, J. Polym. Sci., Polym. Phys. Ed. **16**, 921 (1978).
[47]J. B. Lando and W. W. Doll, J. Macromol. Sci., Phys. B **2**, 205 (1968).


DATE
ILME